Transverse instability of megaripples

Hezi Yizhaq[1], Itzhak Katra[2], Jasper F. Kok[3], and Ori Isenberg[1]
[1]Institute for Dryland Environmental Research, Jacob Blaustein Institutes for Desert Research, Ben-Gurion University of the Negev, Sede Boqer Campus, 84990, Israel
[2] Department of Geography and Environmental Development, Ben-Gurion University of the Negev, Beer Sheva, 84105, Israel
[3]Department of Earth and Atmospheric Sciences, Cornell University, Ithaca, New York, 14853, USA

ABSTRACT

As a result of their inherent differences in stability, sand ripples and megaripples exhibit variations in terms of their wavelengths and grain-size distributions (unimodal for sand ripples and bimodal for megaripples). While sand ripples form almost straight lines, megaripples have greater sinuosity due to their transverse instability, a property that causes small megaripple undulations to grow with time. The origin of the instability is due to variations in megaripple height, variations that do not diminish over time, and due to the inverse dependence of ripple drift velocity on the height. Thus, the taller regions of ripples will move more slowly than the adjacent, shorter portions, an outcome that promotes further perturbation growth. We show an example based on field work of the transverse instability of megaripples. The instability growth rate depends on the difference between the heights of the different segments of the megaripple. In contrast to the underlying instability of megaripples, normal sand ripples are essentially stable and are not affected by transverse perturbations, instead reacting quickly to the wind, which tends to smooth ripple height irregularities. The transverse instability of megaripples derives from the composition of their crests, which comprise coarse particles that allow initial perturbations in ripple height to grow further. The results suggest a physical mechanism for the transverse instability of megaripples and new insight into the spatial patterns of sand ripples.

INTRODUCTION

Eolian ripples, which form regular patterns on sand beaches and desert floors, indicate the fundamental instability of flat sand surfaces under the wind-induced transport of sand grains. Ripples are also found on dunes as part of a hierarchy of bedforms. Two different kinds of sand ripple, normal ripples and megaripples, are observed in nature (Bagnold, 1941; Sharp, 1963). The main features of these ripples are summarized in Table 1. Normal ripples and megaripples have been observed on Mars (Sullivan et al., 2005, 2008; Zimbelman et al., 2009), where eolian processes are also important for understanding the planet's geology (Rubin, 2006). Images from the Mars Global Surveyor clearly portray dust storms, dust devil traces, dunes, and megaripples. Various applications of sand ripple studies on Earth and Mars were reviewed by Rubin (2006).

The physical mechanism responsible for the formation of sand ripples is the action of the wind on loose sand. When the wind strength exceeds some threshold, grains displaced by the direct action of the wind are lifted into the air. However, sand grains are too heavy to be kept aloft even by strong winds, and fall to the ground. During their flight, the grains reach a velocity approximately equal to that of the wind, and upon their impact with the surface, impart energy and momentum to the sand and eject other grains. Under sufficiently high wind velocities, this bombardment by sand grains accelerated by the wind generates a cascade process, resulting in an entire population of saltating grains "hopping" on the sand surface. When the saltating, high-energy grains collide with the bed, they eject reptons, or grains of lower energy (Andreotti, 2004). The windward slopes of small bumps on the sand surface are subjected to more impacts than the lee slopes. The flux of reptons is therefore higher uphill than downhill, which causes the bumps to increase in size.

TABLE 1. MAIN FEATURES OF NORMAL EOLIAN RIPPLES AND MEGARIPPLES

	Normal ripples	Megaripples
Wavelength (λ)	Up to 30 cm	30 cm–43 m
Ripple index*	>15	<15
Formation time scale	Minutes	Days and years
Sorting	Unimodal distribution of grain sizes (typically 0.100–0.300 mm in diameter)	Bimodal distribution of grain sizes, with coarse grains 0.7–4 mm in diameter
Basic process	Saltation and reptation (creep) of fine grains	Saltation and reptation of fine grains and creep of coarse grains
Plan view	Crests form almost straight, continuous lines	Generally, the crests form wavy and discontinuous lines

*Ripple index = ratio of wavelength to height.

Grain-size analyses from different parts of megaripples and from normal ripples show that a bimodal mixture of grain sizes is needed for megaripple formation and that the coarse particles are more abundant at the crest (Yizhaq et al., 2009; Isenberg et al., 2011). Megaripple growth starts with small ripple coalescence. Coarse and fine particles began to segregate, and eventually grain size distributions on the ripple crest became bimodal, and an armored layer of coarse grains covers the crest. The cover of coarse grains on the megaripple crest allows the ripples to grow higher, as strong winds are needed to destroy the cover. In contrast, normal ripples, which are composed only of fine grains, cannot grow higher because weak wind may drive the fine grains at the crest into the saltation cloud (Manukyan and Prigozhin, 2009), thus keeping its height quite low. This is the main difference in the formation process between normal ripples and megaripples. The final wavelength is not simply correlated to the mean saltation length, but rather evolves through interaction between ripples with different sizes. Normal ripples and megaripples exhibit self-organization behavior, where ordered spatiotemporal structures spontaneously emerge (Hallet, 1990; Anderson, 1990; Yizhaq, 2008).

Observations of normal eolian ripples in deserts or on sandy beaches indicate that ripple fields are almost one-dimensional bedforms, and they display only small modulations in the direction transverse to the wind. In this study we report for the first time that megaripples exhibit transverse instability, and suggest a possible mechanism for this instability. The transverse instability increases megaripple sinuosity and increases the merging rate of small ripples; thus the coarsening process becomes faster. Analyzing more quantitatively data from megaripples and ripple sinuosity in different sites will help to better distinguish between these two types of ripples both on Earth and on Mars. Full understanding of this instability will become possible only with a three-dimensional (3-D) megaripple mathematical model, which currently does not exist.

Reffet et al. (2010) showed that transverse dunes are also unstable to transverse perturbations, which break them into barchans. The origin of this instability is differences between

migration rates of valleys (faster) and hills (slower) along the dune crest. We suggest here that a similar mechanism exists for megaripples, although the details are different.

TRANSVERSE INSTABILITY OF MEGARIPPLES

Our field experiment was carried out on the Nahal (wadi) Kasuy sand dunes in the southern Negev that cover an area of 15 km^2. The eolian sand in this area comprises 60% calcite and 35% quartz. Driven by southwestern storm winds, the sand drifts into Nahal Kasuy from the Uvda Valley and accumulates in the wadi bed.

The megaripple mean wavelength in Nahal Kasuy is ~70 cm, and the mean height is ~7 cm (ripple index [defined as the ratio between ripple wavelength and height], RI ~ 10). Smaller ripples reflecting the direction of the most recent wind are superimposed on the megaripples. Compared to megaripples in other parts of the world, those in Nahal Kasuy are small (Fig. 1), and therefore expected to be more sensitive to the storms that form and modify them and can even destroy them (Isenberg et al., 2011).

To study megaripple evolution, we used red-green-blue (RGB) images from a digital Nikon D80 camera with a Sigma 10–20 mm lens. We processed the raw images with Erdas Imagine version 9.1 and its Leica Photogrammetry Software (LPS) extension. The small 10 mm focal length lens provides a 94.5° field of view, which ultimately reduced, relative to using a lens with a larger focal length, the number of photographs needed to cover the plots. To avoid interfering with plot dynamics, the imaging and ground control point markings were made from the area outside the study plots. The camera was mounted on a special rail (5 m long) fixed on each of its ends to a tripod, and could be moved along the rail by two cords attached to the camera body. A remote control cable was used to operate the camera.

The evolution of one megaripple during the period between 17 April 2008 and 8 March 2009 was followed using photographs that documented its instability to transverse perturbation (Fig. 2). The downwind curved portion (bay) of the megaripple expanded over time, which increased the megaripple sinuosity (inferred by the ratio between the bay edge movement to bay vertex movement, which was >1 during the period 17 April 2008–8 March 2009). Because the vertex of the undulation drifted a shorter distance than the edges, an instability developed. These large megaripples were later flattened by strong storms (see Isenberg et al., 2011).

Megaripple drift velocity (celerity) depends both on the wind speed and on ripple height. Wind statistics (measured on site; Isenberg et al., 2011) during this period were used to calculate the drift potential (DP) and the resultant drift potential (RDP) (Fryberger, 1979) (Table 2). Theoretical and empirical studies show that the potential sand volume transported by the wind through a 1-m-wide cross section per unit time is proportional to DP (Fryberger, 1979; Bullard, 1997), calculated from

$$\mathrm{DP} = \left[u^2\left(u - u_t\right)\right], \quad (1)$$

where u is the wind speed (in knots; 1 knot = 0.514 m/s) measured at a height of 10 m and averaged over time, and u_t is the minimal threshold

Figure 1. Normal ripples (foreground) and megaripples (background) in Libyan Desert in Egypt, showing difference in planar patterns of the two bedforms. Normal sand ripples (wavelength, λ = 0.07 m) look almost straight, whereas megaripples (λ = 4 m) in the interdune area are more sinuous, comprising curved segments (prevailing wind direction for megaripples interdune area is from left to right).

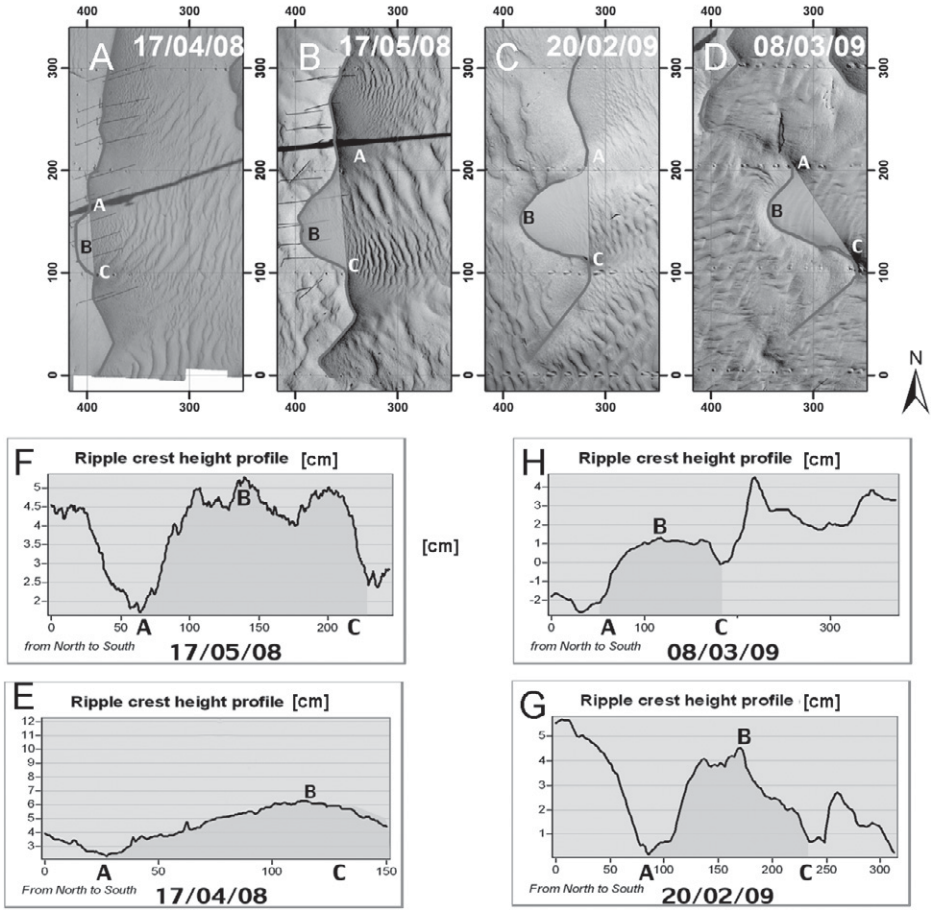

Figure 2. Top: Snapshots of megaripple dynamics show instability to transverse perturbations (prevailing wind direction is from left to right). Curved portion ABC grows over time, increasing megaripple sinuosity. Bottom: Cross sections along line AC of different snapshots (shown at top) illustrating greater ripple height toward inside of downwind curved portion (bay) and shorter height at bay edges. Thus, taller section moved slower than shorter sections, leading to more sinuous megaripple crest over time.

TABLE 2. WIND DATA FROM NAHAL KASUY FOR THE PERIOD 17 APRIL 2008–8 MARCH 2009

Period	DP (v.u.)	RDP (v.u.)	RDD (°)	RDP/DP	*t* (%)
17 April–17 May 2008	5.34	5.18	279	0.94	7.1
18 May 2008–20 February 2008	15.97	7.28	225	0.46	7.38
21 February–8 March 2009	12.99	10.85	251	0.83	18.2

Note: DP is the drift potential; RDP is resultant drift potential; RDD is RDP direction; RDP/DP is the wind directionality and *t* is the time that the wind is above the fluid threshold for sand transport (taken as 6 m/s).

velocity (12 knots) necessary for the transport of typical sand grains (i.e., average diameter of 0.25 mm) (Fryberger, 1979). The direction of RDP is referred to as the resultant drift direction (RDD), which expresses the net trend of sand drift, i.e., the direction in which sand would drift under the influence of winds blowing from various directions, calculated from the vector summation of the DPs from the different directions. The RDP/DP ratio is an index of the directional variability of the wind (RDP/DP = 1 stands for unidirectional wind whereas RDP/DP = 0 characterizes multidirectional winds that vectorially cancel each other).

The bay's growth is correlated to RDP (because this is the net trend of sand drift), and was largest in the period between 20 February 2008 and 8 March 2009, when a strong storm on 27 February registered a wind speed of 15 m/s (at a height of 3.3 m). This storm split the megaripple into two segments (Fig. 2, panel for 8 March 2009).

POTENTIAL MECHANISM FOR TRANSVERSE INSTABILITY

In his seminal book, Bagnold (1941, p. 161, 205) presented a theory of ripple formation predicting that normal ripples are stable to transverse instabilities, i.e., that initially isolated surface irregularities join to form continuous crests perpendicular to the wind. His explanation was based on the assumption that the direction of movement of surface grains (reptons) hit by the saltating grains would vary (inward or outward) along the length of the curved bay-shaped section of the ripple. Thus, different portions of the ripple would advance at different velocities such that a curved ripple portion would eventually straighten to become perpendicular to the prevailing wind. We suggest that megaripple height inconsistencies constitute the origin of megaripple transverse instability. Our findings show that the megaripple was ~4 cm higher along the bay than at its edges (Fig. 2, bottom). Point B, located midway along the curve ABC, was higher than either point A or C. Thus, for the same wind conditions, points A and C moved faster than point B, reflecting the difference in speeds that initiate and increase the transverse perturbation. The lateral sections moved faster than the apex at point B until the megaripple broke down (Fig. 2, panel for 8 March 2009).

Because the megaripple crest is characterized by a layer of coarse particles (median diameter ~700 μm) that are pushed up the incline by the bombardment of fine particles, it can grow higher. The coarse grains exhibit very little lateral creep. Small inconsistencies in megaripple height, therefore, can either grow or decrease slowly, and during this time the megaripple can drift forward and develop a small undulation due to the inverse dependence of the celerity on height.

The average distance of wind-induced megaripple migration and the wind speed measurements allowed us to calculate the creep mass flux of the coarse particles q_c (Jerolmack et al., 2006; Zimbelman et al., 2009):

$$q_c = (1-p)\rho c H/2, \quad (2)$$

where p is the porosity, ρ is the particle density, c is the ripple migration rate, and H is the ripple height. Entailed in using Equation 2 is the assumption that ripple height remains unchanged, and assuming triangular shapes (Anderson, 1990). It follows that $c = 2q_c/[(1-p)\rho H]$, and thus the rate of growth of the transverse instability will be dictated by the difference in the migration speeds (c_1 and c_2) of the two megaripple sections given by:

$$\frac{\Delta x}{\Delta t} = c_1 - c_2 = \frac{2q_c(H_2 - H_1)}{(1-p)\rho H_1 H_2}, \quad (3)$$

where H_1 is the height of the edges, H_2 is the height of the vertex, and Δt is the time interval between two successive snapshots. According to Equation 3, the larger the difference in height, the larger the instability in the growth rate. In our previous work (Isenberg et al., 2011), we estimated the averaged flux of the coarse particles during the period 21 February–8 March 2009 as $q_c = 9.49 \times 10^{-6}$ kg m^{-1}s^{-1}. Using this value and $p = 0.35$, ρ = 2710 kg m^{-3}, and assuming that $H_1 = 0.04$ m and $H_2 = 0.08$ m, we can estimate the difference between the distances moved by the edges and that of the apex via $\Delta x = (c_2 - c_1)\Delta t$, where $\Delta t = 18$ days. This calculation gives 18.62 cm, which is in agreement with the measured distance of 17 cm (see Table 3).

DISCUSSION AND CONCLUSIONS

We showed that whereas normal ripples appear to be stable, megaripples are laterally unstable, resulting in the behavior that is responsible for the different planar appearances of the two ripple forms (Fig. 1). We explain megaripple instability through the differences in the drift velocities of ripple sections along the crest, which differ in their heights. Nonuniform megaripple height may be due to irregularities in the accumulation of coarse particles (both number and sizes) and deviations in wind direction. In contrast to megaripples, normal ripples are laterally stable, since fluctuations in their heights are quickly diminished. This is shown in a 3-D mathematical model (Yizhaq et al., 2004) of normal sand ripples based on Anderson's (1987) idea that ripples develop due to spatial differences in the reptation flux and that the role of saltation is merely to introduce energy into the system. The lateral divergence of the flux is modeled by a diffusion term that smooths any perturbations in ripple height. During normal ripple evolution (Fig. 3), ripples spread laterally and crests tend to become parallel, indicating stability with respect to perturbations in the transverse direction.

Unfortunately, there is no 3-D model of megaripples that we can use to validate our explanation. Instead, we use a recently developed numerical model of saltation known as COMSALT (Kok and Renno, 2009) to study the difference between the reptation flux of normal ripples (with a unimodal 180 μm size distribution) and megaripples (with a bimodal grain size distribution of 50% 180 μm and 50% 700 μm sand by surface area) with a grain size distribution that represents the ripples at Nahal Kasuy (Isenberg et al., 2011). These simulations are shown in Figure 4 and demonstrate that the much larger inertia of the coarse megaripple grains causes their creep to be one to two orders of magnitude less than that of the normal ripple.

TABLE 3. SIZE PARAMETERS OF THE MEGARIPPLE FOR 17 APRIL 2008–8 MARCH 2009

Date	Bay width* (cm)	Bay vertex movement (cm)	Bay average edge movement (cm)	Bay area (cm²)
17 April 2008	73			782
18 April–17 May 2008	108	19	44	2798
18 May 2008–-20 February 2009	101	14	24	4055
21 February–8 March 2009	112	38	55	2831

*Bay is downward curved portion of ripple.

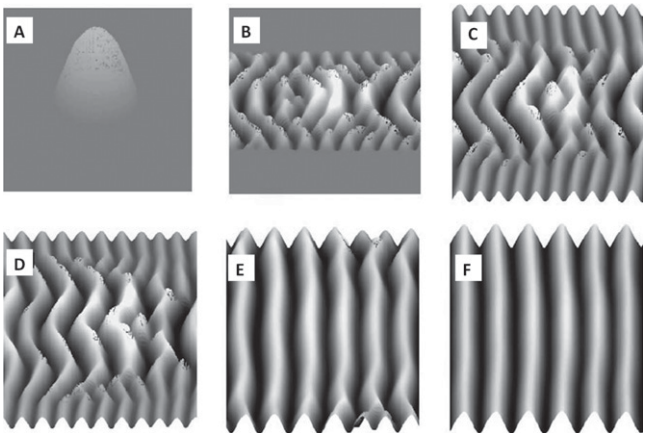

Figure 3. Simulated ripples initiated from small Gaussian hump (wind direction is from left to right). After a short time, initial pile generates array of ripples. Note that because of periodic boundary conditions, when ripples cross right edge of simulation box, they reenter from left side. See Yizhaq et al. (2004) for more details of mathematical model.

In a similar manner, it was theoretically shown (Niiya et al., 2010) that the amount of lateral diffusion governs the stability of transverse dunes to lateral perturbations.

The results suggest a physical mechanism for the instability of megaripples. Relevant future questions include (1) are the coarser particles more abundant on the higher parts along the crest of the megaripples than on the lower parts of the crest, and (2) is there a systematic relation between the orientation of the bay (forward or backward vis-à-vis wind direction) and the direction of megaripple advance, i.e., does the bay remain behind or in front of the other parts of the crest? Long-term studies of megaripple evolution and morphodynamics are needed to confirm our conclusions and test our hypothesis about the morphodynamics of megaripple fields.

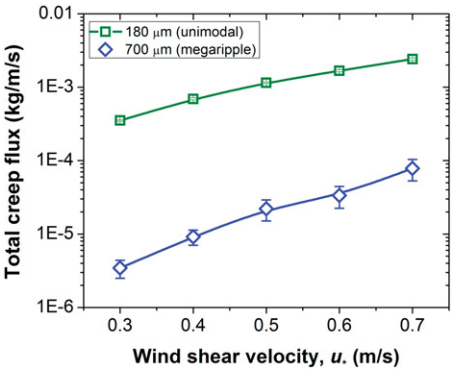

Figure 4. Simulations with numerical saltation model COMSALT (Kok and Renno, 2009) of creep flux as function of wind shear velocity (square root of wind stress divided by air density) for both normal (180 μm) ripple and coarse fraction (700 μm) of megaripple. Model defines creep flux as flux of ejected particles that, upon impact on surface, does not rebound.

ACKNOWLEDGMENTS

This work was supported by the Israel Science Foundation (grant N531/06).

REFERENCES CITED

Anderson, R.S., 1987, A theoretical model for aeolian impact ripples: Sedimentology, v. 34, p. 943–956, doi:10.1111/j.1365-3091.1987.tb00814.x.

Anderson, R.S., 1990, Eolian ripples as example of self-organization in geomorphological systems: Earth Science Reviews, v. 29, p. 77–96, doi:10.1016/0012-8252(90)90029-U.

Andreotti, B., 2004, A two-species model of aeolian sand transport: Journal of Fluid Mechanics, v. 510, p. 47–70, doi:10.1017/S0022112004009073.

Bagnold, R.A., 1941, The physics of blown sand and desert dunes: London, Methuen, 265 p.

Bullard, J.E., 1997, A note on the use of the "Fryberger method" for evaluating potential sand transport by wind: Sedimentary Research, v. 67, p. 499–501.

Fryberger, S.G., 1979, Dune forms and wind regime, *in* McKee, E.D., ed., A study of global sand seas: U.S. Geological Survey Profile Paper 1052, p. 137–169.

Hallet, B., 1990, Spatial self-organization in geomorphology: From periodic bedforms and patterned ground to scale-invariant topography: Earth Science Reviews, v. 29, p. 57–76, doi:10.1016/0012-8252(0)90028-T.

Isenberg, O., Yizhaq, H., Tsoar, H., Wenkart, R., Karnieli, A., Kok, J., and Katra, I., 2011, Megaripple flattening due to strong winds: Geomorphology, v. 131, p. 69–84.

Jerolmack, D.J., Mohrig, D., Grootzinger, J.P., Fike, D., and Watters, W.A., 2006, Spatial grain size sorting in eolian ripples and estimation of wind conditions on planetary surfaces: Application to Meridiani Planum, Mars: Journal of Geophysical Research, v. 111, E12S02, doi:10.1029/2005JE002544.

Kok, J.F., and Renno, N.O., 2009, A comprehensive numerical model of steady state saltation (COMSALT): Journal of Geophysical Research, v. 114, D17204, doi:10.1029/2009JD011702.

Manukyan, E., and Prigozhin, L., 2009, Formation of aeolian ripples and sand sorting: Physical Review E: Statistical, Nonlinear, and Soft Matter Physics, v. 79, 031303, doi:10.1103/PhysRevE.79.031303.

Niiya, H., Awazu, A., and Nishimori, H., 2010, Three-dimensional dune skeleton model as a coupled dynamical system of two-dimensional cross sections: Physical Society of Japan Journal, v. 79, 063002, doi:10.1143/JPSJ.79.063002.

Reffet, E., Courrech du Pont, S., Hersen, P., and Douady, S., 2010, Formation and stability of transverse and longitudinal sand dunes: Geology, v. 38, p. 491–494, doi:10.1130/G30894.1.

Rubin, D.M., 2006, Ripple effect: Unforeseen applications of sand studies: Eos (Transactions, American Geophysical Union), v. 87, p. 293, 297.

Sharp, R.P., 1963, Wind ripples: Journal of Geology, v. 71, p. 617–636, doi:10.1086/626936.

Sullivan, R., and 17 others, 2005, Aeolian processes at the Mars Exploration Rover Meridiani Planum landing site: Nature, v. 436, p. 58–61, doi:10.1038/nature03641.

Sullivan, R., Arvidson, R., Bell, J.F., Gellert, R., Golombek, M., Greeley, R., Herkenhoff, K., Johnson, J., Thompson, S., Whelley, P., and Wray, J., 2008, Wind-driven particle mobility on Mars: Insights from Mars Exploration Rover observations at "El Dorado" and surroundings at Gusev crater: Journal of Geophysical Research, v. 113, E06S07, doi:10.1029/2008JE003101.

Yizhaq, H., 2008, Aeolian megaripples: Mathematical model and numerical simulations: Journal of Coastal Research, v. 24, p. 1369–1378, doi:10.2112/08A-0012.1.

Yizhaq, H., Balmorth, N., and Provenzale, A., 2004, Blown by wind: Nonlinear dynamics of aeolian sand ripples: Physica D, Nonlinear Phenomena, v. 195, p. 207–228, doi:10.1016/j.physd.2004.03.015.

Yizhaq, H., Isenberg, O., Wenkart, R., Tsoar, H., and Karnieli, A., 2009, Morphology and dynamics of aeolian megaripples in Nahal Kasuy, southern Israel: Israel Journal of Earth Sciences, v. 57, p. 145–161.

Zimbelman, J.R., Irwin, R.P., III, Williams, S.H., Bunch, F., Valdez, A., and Stevens, S., 2009, The rate of granule ripples movement on Earth and Mars: Icarus, v. 203, p. 71–76, doi:10.1016/j.icarus.2009.03.033.

Manuscript received 3 November 2011
Revised manuscript received 1 January 2012
Manuscript accepted 5 January 2012

Printed in USA